

THEORETICAL STUDY OF THE PH₃-ASSISTED MIGRATION OF A COORDINATED ARYL GROUP TO A COORDINATED CO IN THE COMPLEXES RhCpI(CO)(p-XC₆H₄)

NASRIN SADEGHI¹, REZA GHIASI², *, SAEID JAMEHBOZORG³

¹Department of Chemistry, Faculty of science, Arak Branch, Islamic Azad University, Arak, Iran

²Department of Chemistry, East Tehran Branch, Islamic Azad University, Qiam Dasht, Tehran, Iran

³Department of chemistry, Faculty of Basic Science, Hamedan Branch, Islamic Azad University, Hamedan, Iran

ABSTRACT

We report the results of theoretical mechanistic studies on PH₃-assisted migration of a coordinated aryl group to a coordinated CO in the complexes RhCpI(CO)(p-XC₆H₄). The X-substituent effect on thermodynamic and kinetic parameters was explored. The progress of the reaction was quantitatively studied using the bond orders of the Rh-CO bond, and the percentages of bond cleavage (BC_i) of Rh-CO bond at the transition state were described. This theoretical study indicates good relationships between barrier energy (ΔE), bond distances variations (Rh-CO and Rh-Ph), activation energy (ΔH[‡]), activation free energy (ΔG[‡]) values with Hammett constants of X-substituents. Linear relationship between ln(k) and the ¹⁰³Rh magnetic shielding tensors of the product was explored.

Keyword: Insertion reaction, Substituent effect, Thermodynamic parameters, Kinetic parameters.

INTRODUCTION

Migratory insertion reactions have enormous value in organometallic chemistry [1] and are concerned in a variety of catalytic processes, both homogeneous and heterogeneous. The migration of a coordinated organic group R onto a co-ordinated carbonyl of a metal promoted by an entering ligand (nucleophile) has been widely studied for systems such as [RMn(CO)₅] [2-4], [(Cp)FeR(CO)₂] [5-8] or [(Cp)MoR(CO)₃] [9-12]. Also, theoretical studies have given important information on the nature of the migratory insertion process [13-18].

The PPh₃-assisted migration of a coordinated aryl group to a coordinated CO in the complexes RhCp*I[(CO)(p-XC₆H₄)]PPh₃ reported [19]. It was found that the mechanism was associative and solvent independent [20], and it is also possible that ring slippage is not involved [21,22]. Also, correlation of the transition-metal chemical shifts of the product with reaction rates has been reported and leads to the postulate that such reactions are characterized by a product-like (late) transition state [23].

On the basis of the major effects that substituents afford to a wide range of chemical properties, e.g. reaction rates, structural parameters, thermodynamic parameters and so on, it is proper to visualize a situation where the thoughtful selection of a proper substituent could make the variation between an effective and ineffective receptor. Hence, an in depth exploring of substituent effects and their origins might allow the proposing of a new receptor that has been wily tuned for the best preferred performance.

In this study, we investigate theoretically the PH₃-assisted migration of a coordinated aryl group to a coordinated CO in the complexes RhCpI(CO)(p-XC₆H₄) and hope to clarify the substitution effect on their activation barriers and thermodynamics of these insertion reactions.

Computational Methods

All calculations were performed with the Gaussian 09 suite of program [24]. The calculations of systems contain C, H, P, N, F, Cl, I and O described by the standard 6-311G(d,p) basis set [25-28]. For Rh element standard Def2-TZVPPD basis set [29] was used and Rh described by effective core potential (ECP) of Wadt and Hay pseudo-potential with using the Def2-TZVPPD basis set [30]. Geometry optimization was varied out with Modified Perdew-Wang Exchange and Correlation (mpw1pw91) [31]. To verifying that the optimization structures are minima, harmonic vibrational frequencies were calculated. All the transition states were checked by IRC (Intrinsic Reaction Coordinate) analysis [32-35].

¹⁰³Rh magnetic shielding tensors are calculated using the Gauge independent atomic orbital (GIAO) [36] method at the same method and basis sets for optimization.

RESULTS AND DISCUSSION

Figure 1 exhibits the mechanism of insertion reaction in CpRh(CO)I(p-XC₆H₄) (I) complex in the presence of PH₃. Mechanistic studies on the reaction of CpRh(CO)I(p-XC₆H₄) with PH₃ suggest it proceeds through an initial five-coordinate PH₃ adduct from which intramolecular migratory insertion can then occur.

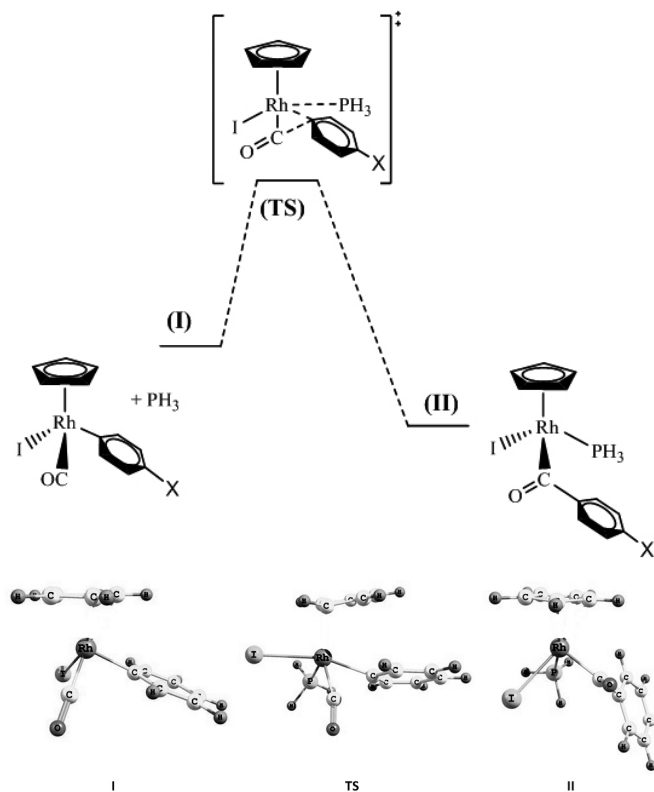


Figure 1. Mechanism of migratory insertion reaction in CpRh(CO) I (p-C₆H₄X) + PH₃ reaction.

1. Energetic aspects.

The absolute, Zero-point correction, and relative energies values of reactants, transition states and products complexes in gas phase are gathered in Tables 1a-b.

Table 1. (a) Energy (Hartree), Zero-point correction (Hartree) and (b) energy barrier (kcal/mol), corrected relative energy (kcal/mol) values of the I, Ts and II structures and Hammett constant of substituents (σ_p). For PH_3 , $E=-343.1633323$ (Hartree), and Zero-point correction 0.024125 (Hartree).

(a)

X	σ_p	E			Zero-point correction		
		I	TS	II	I	TS	II
NH ₂	-0.66	-7624.5298	-7967.6497	-7967.7199	0.201692	0.227990	0.231466
OH	-0.37	-7644.3948	-7987.5124	-7987.5835	0.189285	0.215738	0.219060
Me	-0.17	-7608.4883	-7951.6035	-7951.6753	0.212351	0.238599	0.241990
H	0.00	-7569.1702	-7912.2842	-7912.3564	0.185011	0.211248	0.214688
F	0.06	-7668.4118	-8011.5263	-8011.5981	0.176826	0.203055	0.206410
Cl	0.23	-8028.8009	-8371.9140	-8371.9864	0.175436	0.201594	0.205122
CHO	0.42	-7682.4956	-8025.6060	-8025.6791	0.194416	0.220404	0.223924
COOH	0.45	-7757.7549	-8100.8660	-8100.9391	0.200424	0.226565	0.230111
NO ₂	0.78	-7773.6771	-8116.7864	-8116.8601	0.187905	0.213927	0.217496

(b)

X	I	TS	II
NH ₂	0.00	28.617759	-13.2521849
OH	0.00	30.1582948	-12.3730441
Me	0.00	31.5356782	-11.3916192
H	0.00	32.281787	-10.8657662
F	0.00	31.9630121	-10.9868756
Cl	0.00	32.7969723	-10.420862
CHO	0.00	34.3845713	-9.27753971
COOH	0.00	34.0413236	-9.60447215
NO ₂	0.00	35.0961671	-8.91170167

Hessian calculations illustrate positive vibrational frequencies for reactants and products species given in Figures S1, signifying that they locate on minima in the potential energy surface.

Transition state shown in Figure 1 has only one imaginary vibrational frequency, verifying that it is a first-order saddle point in the PES. The calculated imaginary frequency of transition states are gathered in Table 2. The IRC calculations displayed that the TSs connected the reactants and the product.

Table2. Selected bond distances in I, Ts and II structures (in Å) and Imaginary frequency of transition states (ν_{IMG} in cm^{-1}).

X	Rh-CO			Rh-Ph			Rh-PH ₃		ν_{IMG}
	I	TS	II	I	TS	TS	II		
NH ₂	1.850	1.835	2.035	2.062	2.165	2.274	2.259	-293.7524	
OH	1.851	1.835	2.030	2.060	2.184	2.274	2.262	-299.7035	
Me	1.852	1.834	2.026	2.059	2.203	2.274	2.263	-309.8166	
H	1.852	1.835	2.024	2.060	2.216	2.273	2.264	-315.3920	
F	1.854	1.835	2.027	2.059	2.206	2.275	2.264	-308.7880	
Cl	1.855	1.835	2.023	2.057	2.216	2.275	2.265	-315.3433	
CHO	1.857	1.835	2.021	2.053	2.237	2.274	2.266	-328.6332	
COOH	1.856	1.834	2.021	2.054	2.233	2.276	2.265	-324.4861	
NO ₂	1.858	1.835	2.019	2.052	2.246	2.276	2.267	-329.1886	

As we can see from Table 1(b), the energy barrier values, $\Delta E=E(\text{TS})-[E(\text{I})+E(\text{PH}_3)]$, of insertion reaction decrease in the presence of donor-electron groups.

The Hammett equation (and its extended forms) is the most extensively used means for the investigation and explanation of reactions and their mechanisms. Hammett constants σ_m and σ_p (for substituent in m and

p-positions, respectively) provided from ionization of organic acids in solutions can commonly successfully predict equilibrium and rate constants for many reactions [37]. The study of energy and Hammett constant in this insertion reaction show that a good linear relationship between two parameters:

$$\text{Barrier energy} = 4.590 \sigma_p + 31.94;$$

$$R^2 = 0.973$$

2. Geometrical parameters

Selected bond distances of reactant, transition state, and products complexes are gathered in Table 2. The bond distances values reveal in the optimized geometry of the transition state **TS** the Rh-Ph bond is weakened. The range of weakness of this bond increases in the presence of withdrawing electron substitutions. A good linear relationship is observed between $\Delta r_{\text{Rh-Ph}} = r(\text{Rh-Ph})_{\text{TS}} - r(\text{Rh-Ph})_I$ and Hammett constant:

$$\Delta r_{\text{Rh-Ph}} = 0.064\sigma_p + 0.149; \quad R^2 = 0.963$$

On the other hand, the optimized geometry of the transition state **TS** reveals that Rh-CO bond length decreases. There is a good linear relationship between $\Delta r_{\text{Rh-CO}} = r(\text{Rh-CO})_I - r(\text{Rh-CO})_{\text{TS}}$ and Hammett constant:

$$\Delta r_{\text{Rh-CO}} = 0.006\sigma_p + 0.018; \quad R^2 = 0.933$$

The variations of Rh-CO bond lengths are less than Rh-Ph bond. The range of reinforce of this bond increases in the presence of withdrawing electron substitutions.

The progress of the reaction has been quantitatively monitored using the bond orders of the above bonds. The percentages of bond formation (BF_{ij}) and cleavage (BC_{ij}) at the transition state have been described by Manoharan and Venuvanalingam as [38,39]:

In this equation, ρ is the bond order at the transition state, and ρ_I and ρ_{II} correspond to the bond orders at the reactant and the product stages, respectively.

The computed Wiberg bond indices [40], of Rh-CO bond are summarized in Table 3. The bond order values of Rh-CO are 1.0487, 0.9733, and 0.7483 in **I**, **TS**, and **II** structures, respectively. Therefore, in the transition state **TS**, the cleavage of π -bonding along the Rh-CO bond is 25.1%. On the other

hand, these values decrease in the presence of donor and withdrawing electron groups.

Table 3. Bond order and percentages of cleavage (BC_{ij}) of Rh-CO at the transition state in insertion reaction.

X	I	TS	II	$BC_{\text{Rh-CO}}$
NH₂	1.0511	0.9767	0.7346	23.51
OH	1.0509	0.9754	0.7412	24.38
Me	1.0498	0.9741	0.7457	24.89
H	1.0487	0.9733	0.7483	25.10
F	1.0470	0.9744	0.7468	24.18
Cl	1.0458	0.9734	0.7501	24.48
CHO	1.0419	0.9717	0.7528	24.28
COOH	1.0442	0.9735	0.7526	24.25
NO₂	1.0408	0.9728	0.7563	23.90

3. Thermodynamic parameters

The values of free energies of insertion reaction are gathered in Table 4. These values indicate activation free energy values (ΔG^\ddagger) increase in the presence of withdrawing electron groups (X=COOH, CHO, NO₂). Figure 2 shows a good relationship between ΔG^\ddagger and Hammett constant of substituents.

$$\Delta G^\ddagger = 4.283\sigma_p + 42.79; \quad R^2 = 0.972$$

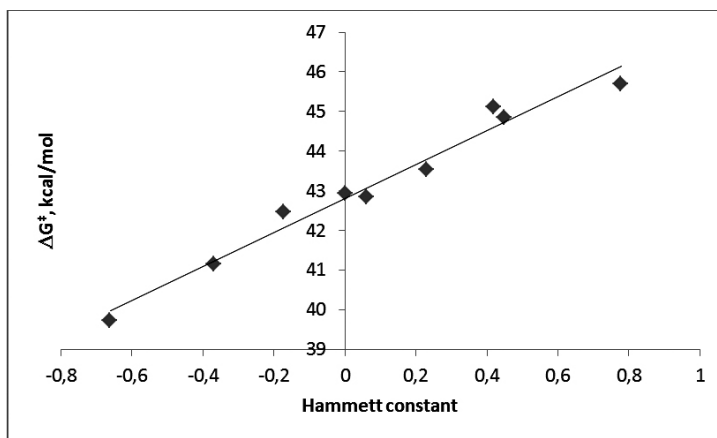


Figure 2. Relationship between ΔG^\ddagger and Hammett constant.

Table 4. Free energy values in the I, Ts and II structures (in a.u), activation free energy (ΔG^\ddagger , kcal/mol), rate constant (k , s⁻¹), free energy of insertion reaction ($\Delta G^{\text{insertion}}$, kcal/mol).

X	I	G	II	ΔG^\ddagger	k	$\Delta G^{\text{insertion}}$
	I	TS	II	TS		II
NH₂	-7624.3752	-7967.4711	-7967.5377	39.72	4.63×10^{-17}	-2.09
OH	-7644.2522	-7987.3459	-7987.4136	41.14	4.22×10^{-18}	-1.34
Me	-7608.3243	-7951.4159	-7951.4848	42.47	4.46×10^{-19}	-0.80
H	-7569.0301	-7912.1209	-7912.1901	42.91	2.10×10^{-19}	-0.54
F	-7668.2815	-8011.3724	-8011.4410	42.87	2.26×10^{-19}	-0.14
Cl	-8028.6727	-8371.7625	-8371.8312	43.55	7.20×10^{-20}	0.48
CHO	-7682.3493	-8025.4366	-8025.5060	45.13	4.93×10^{-21}	1.59
COOH	-7757.6040	-8100.6918	-8100.7609	44.84	8.02×10^{-21}	1.45
NO₂	-7773.5385	-8116.6249	-8116.6947	45.70	1.90×10^{-21}	1.87

The free energies change values of insertion reaction ($\Delta G^{\text{insertion}}$) illustrates that insertion reaction is more favorable thermodynamically in the presence of donor electron groups ($X=\text{OH}, \text{NH}_2, \text{Me}$). On the other hand, these values exhibit that insertion reaction is more unfavorable thermodynamically in the presence of withdrawing electron groups ($X=\text{COOH}, \text{CHO}, \text{NO}_2$).

The values of activation enthalpy (ΔH^\ddagger) of insertion reaction are presented

in Table 5. One can see from Table 5, these values increase in the presence of withdrawing electron groups ($X=\text{COOH}, \text{CHO}, \text{NO}_2$). Figure 3 shows a good relationship between ΔH^\ddagger and Hammett constant of substituents.

$$\Delta H^\ddagger = 4.657 \sigma_p + 31.27;$$

$$R^2 = 0.972$$

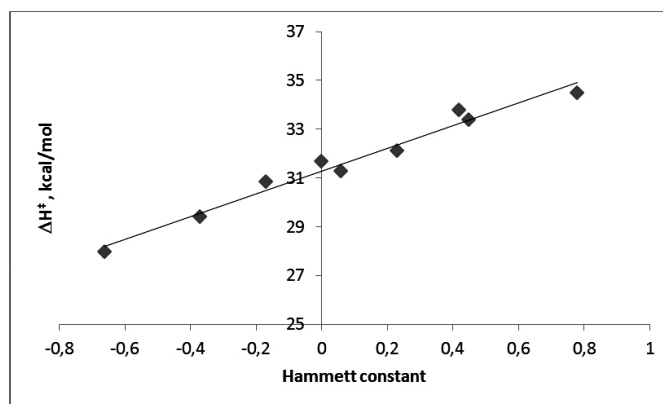


Figure 3. Relationship between ΔH^\ddagger and Hammett constant.

Table 5. Enthalpy values in the I, Ts and II structures (in a.u.), activation enthalpy (ΔG^\ddagger , kcal/mol), enthalpy of insertion reaction ($\Delta G^{\text{insertion}}$, kcal/mol).

X	H			ΔH^\ddagger		$\Delta H^{\text{insertion}}$
	I	TS	II	TS	II	
NH ₂	-7624.3110	-7967.4018	-7967.4690	27.96	-14.17	
OH	-7644.1887	-7987.2772	-7987.3453	29.39	-13.33	
Me	-7608.2584	-7951.3446	-7951.4133	30.85	-12.26	
H	-7568.9697	-7912.0545	-7912.1237	31.67	-11.73	
F	-7668.2186	-8011.3041	-8011.3729	31.29	-11.89	
Cl	-8028.6086	-8371.6928	-8371.7620	32.12	-11.33	
CHO	-7682.2836	-8025.3651	-8025.4351	33.77	-10.15	
COOH	-7757.5360	-8100.6181	-8100.6881	33.39	-10.52	
NO ₂	-7773.4711	-8116.5515	-8116.6220	34.49	-9.78	

Table 6. ¹⁰³Rh Magnetic shielding tensor for the I, Ts and II structures.

X	I	TS	II
NH ₂	-304.7834	-477.8827	-396.8823
OH	-302.6120	-478.9506	-392.7003
Me	-303.1460	-481.1645	-391.5912
H	-304.0996	-483.7588	-389.6798
F	-301.1357	-481.4023	-387.6321
Cl	-299.2582	-482.7937	-385.7659
CHO	-300.6179	-487.1724	-382.7392
COOH	-300.4044	-486.6029	-384.4457
NO ₂	-296.8597	-489.5353	-378.4133

The enthalpy change values of insertion reaction ($\Delta H^{\text{insertion}}$) illustrates that these values are less in the presence of withdrawing electron groups ($X=\text{COOH}, \text{CHO}, \text{NO}_2$).

4. Rate constant values

Rate constants are estimated by canonical TS theory using Eyring equation [41-43]:

In this equation, k_b is the Boltzmann's constant, h is the Planck's constant, T is the temperature, R is the ideal gas constant, ΔG^\ddagger is the activation barrier at 298 K.

The rate constant values of insertion reactions are gathered in Table 4. These values show that rate constant values are more in the presence of donor electron groups ($X=\text{OH}, \text{NH}_2, \text{Me}$). These values show linear dependence between $\ln(k)$ values and Hammett constants:

$$\ln(k) = -7.235 \sigma_p - 42.80; \quad R^2 = 0.972$$

5.¹⁰³Rh Magnetic shielding tensor

¹⁰³Rh Magnetic shielding tensors (σ) of the I, Ts and II structures are given in Table 6. One can see from Table 6, these values decrease in transition state rather than reactant complex. A good linear relationship between $\sigma_{TS} - \sigma_I$ values and the Hammett constant of the substituents is observed:

$$\sigma_{TS} - \sigma_I = -13.35 \sigma_p - 180.7; \quad R^2 = 0.974$$

On the other hand, there is a good linear relationship between $\ln(k)$ and the ¹⁰³Rh magnetic shielding tensors (σ_{Rh}) of the product rather than of the reactant:

$$\begin{aligned} \text{Product: } \sigma_{Rh} &= 1.152 \ln(k) - 433.2; & R^2 &= 0.931 \\ \text{Reactant: } \sigma_{Rh} &= -0.623 \ln(k) - 328.4; & R^2 &= 0.661 \end{aligned}$$

Therefore, the aryl migration proceeds via a late transition state, which is structurally more similar to the product than the reactant [23]. This illustrates in the transition state the Ph-C(O) and Rh-P bonds are already formed to an significant amount with simultaneous breaking of the Rh-Ph bond. Thus, complete breakage of the Rh-Ph bond and formation of the Rh-P bond leads to the final product.

CONCLUSION

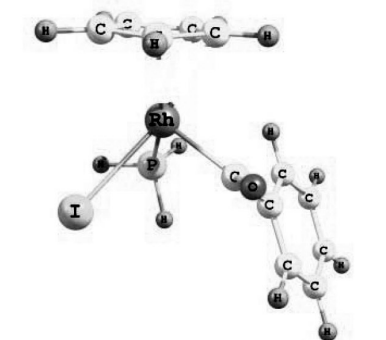
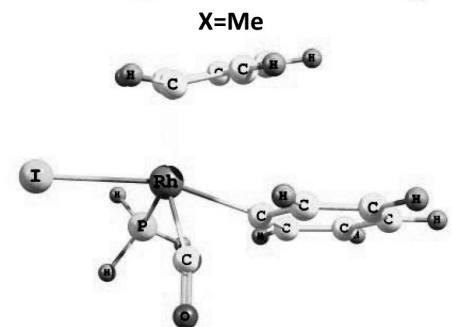
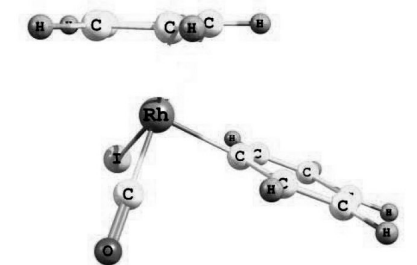
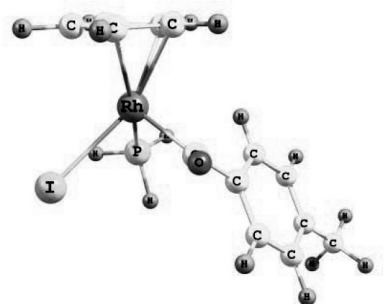
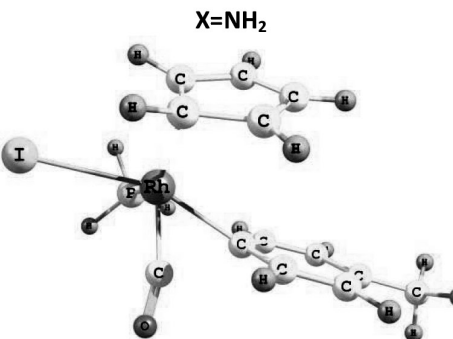
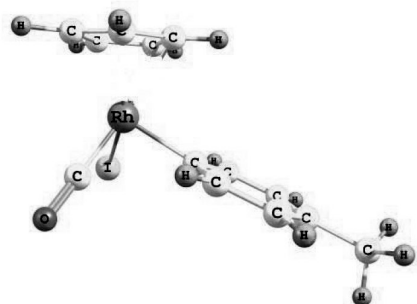
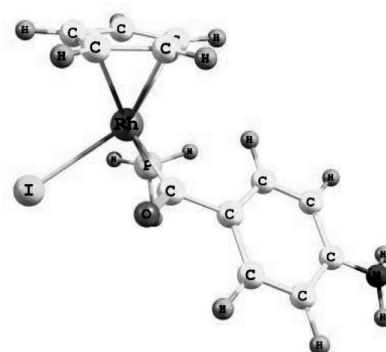
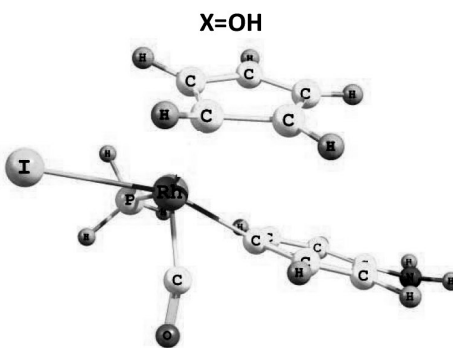
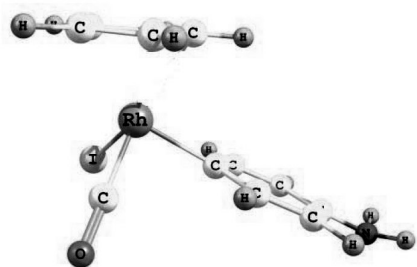
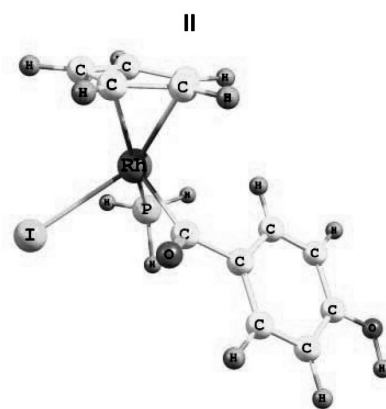
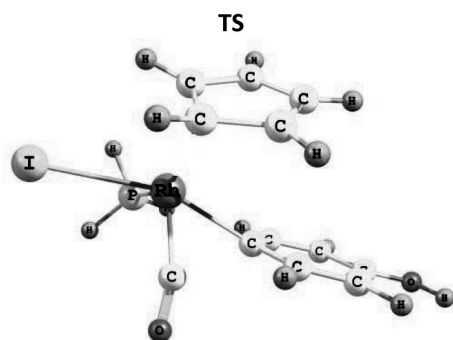
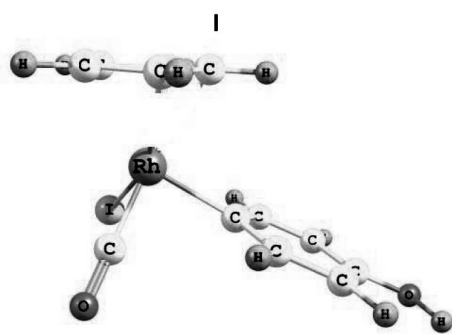
In this paper, we investigated the insertion reactions of the PH₃-assisted migration of a coordinated aryl group to a coordinated CO in the complexes RhCpI(CO)(p-XC₆H₄) by computational method. The theoretical calculations predicted:

1. The character of X-substituents influences energetic, thermodynamic and kinetic parameters of the reaction.
2. The energy barriers (E=E(TS)-E(I)) in the presence of withdrawing electron groups are higher than those in donor electron groups.
3. There are good linear relationships between variation of Rh-Ph, and Rh-CO bond distances with Hammett constants.
4. The free energies change values of insertion reaction ($\Delta G^{\text{insertion}}$) show that insertion reaction is more favorable thermodynamically in the presence of donor electron groups (X=OH, NH₂, Me).
5. In the transition state TS, the cleavage of π -bonding along the Rh-CO bond decrease in the presence of donor and withdrawing electron groups.
6. Rate constant values increase in the presence of donor electron groups (X=OH, NH₂, Me).
7. A good linear relationship between $\ln(k)$ and the ¹⁰³Rh magnetic shielding tensors of the product explores aryl migration proceeds via a transition state, which is structurally more similar to the product than the reactant.

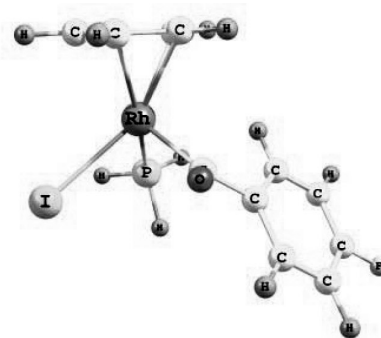
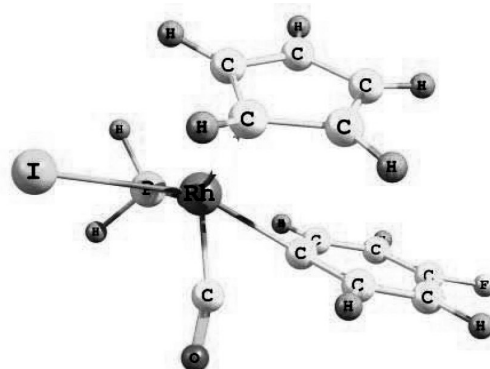
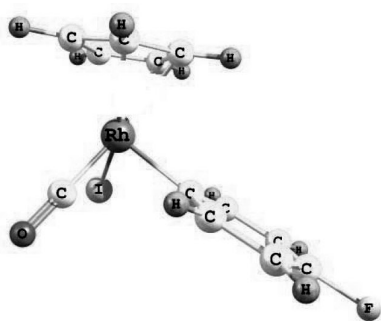
REFERENCES

1. G. L. Meissler, D. A. Tarr: *Inorganic Chemistry*; Prentice Hall: Upper Saddle River, 2004.
2. R. J. Mawby, F. Basolo, R. G. Pearson, *J. Am. Chem. Soc.* **1964**, *86*, 3994.
3. J. D. Cotton, R. D. Markwell, *Organometallics* **1985**, *4*, 937.
4. J. N. Cawse, R. A. Fiato, R. L. Pruett, *J. Organomet. Chem.* **1979**, *172*, 405.
5. I. S. Butler, F. Basolo, R. G. Pearson, *Inorg. Chem.* **1967**, *6*, 2074.
6. K. Nicholas, S. Raghunathan, M. Rosenblum, *J. Organomet. Chem.* **1974**, *78*, 133.
7. J. D. Cotton, G. T. Crisp, L. Latif, *Inorg. Chim. Acta.* **1981**, *47*, 171.
8. C. R. Jablonski, Y. P. Wang, *Inorg. Chim. Acta.* **1983**, *69*, 147.
9. P. J. Craig, M. Green, *J. Chem. Soc. A* **1968**, 1978.
10. M. J. Wax, R. G. Bergman, *J. Am. Chem. Soc.* **1981**, *103*, 7028.
11. J. D. Cotton, H. A. Kimlin, *J. Organomet. Chem.* **1985**, *294*, 213.
12. J. D. Cotton, G. T. Crisp, V. A. Daly, *Inorg. Chim. Acta.* **1981**, *47*, 165.
13. H. Berke, R. Hoffmann, *J. Am. Chem. Soc.* **1978**, *100*, 7224.
14. S. Sakaki, K. Kitaura, K. Morokuma, K. Ohkubo, *J. Am. Chem. Soc.* **1983**, *105*, 2280.
15. C. D. Montgomery, *J. Chem. Educ.* **2013**, *90*, 1396.
16. W.-Z. Li, B.-F. Yan, Q.-Z. Li, J.-B. Cheng, *Journal of Organometallic Chemistry* **2013**, *724*, 163.
17. X. Wang, E. Weitz, *Journal of Organometallic Chemistry* **2004**, *689*, 2354.
18. X. Wang, E. Weitz, *J. Phys. Chem. A* **2002**, *106*, 11782.
19. M. Bassetti, G. J. Sunley, F. P. Fanizzi, P. M. Maitlis, **1990**, 1799.
20. M. Bassetti, G. J. Sunley, P. M. Maitlis, *J. Chem. Soc., Chem. Commun.* **1988**, 1012.
21. M. Bassetti, L. Mannina, D. Monti, *Organometallics* **1994**, *13*, 3293.

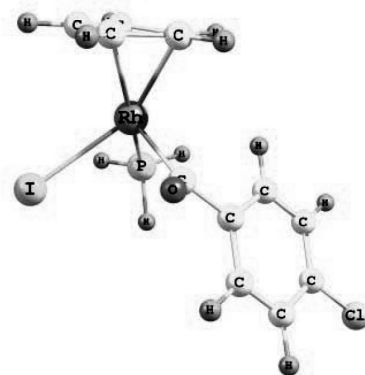
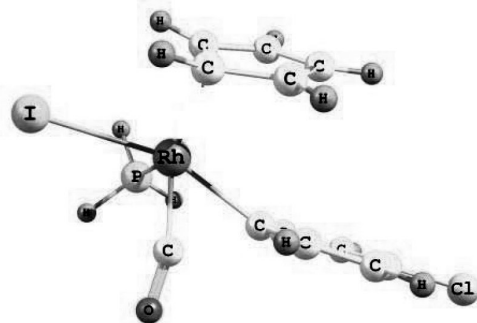
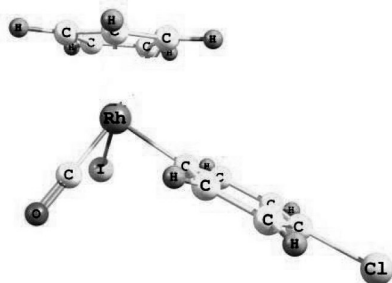
22. D. Monti, M. Bassetti, *J. Am. Chem. Soc.* **1993**, *115*, 4658.
23. V. Tedesco, W. v. Philipsborn, *Organometallics* **1995**, *14*, 3600.
24. M. J. Frisch, G. W. Trucks, H. B. Schlegel, G. E. Scuseria, M. A. Robb, J. R. Cheeseman, G. Scalman, V. Barone, B. Mennucci, G. A. Petersson, H. Nakatsuji, M. Caricato, X. Li, H. P. Hratchian, A. F. Izmaylov, J. Bloino, G. Zheng, J. L. Sonnenberg, M. Hada, M. Ehara, K. Toyota, R. Fukuda, J. Hasegawa, M. Ishida, T. Nakajima, Y. Honda, O. Kitao, H. Nakai, T. Vreven, J. A. Montgomery, Jr., J. E. Peralta, F. Ogliaro, M. Bearpark, J. J. Heyd, E. Brothers, K. N. Kudin, V. N. Staroverov, R. Kobayashi, J. Normand, K. Raghavachari, A. Rendell, J. C. Burant, S. S. Iyengar, J. Tomasi, M. Cossi, N. Rega, J. M. Millam, M. Klene, J. E. Knox, J. B. Cross, V. Bakken, C. Adamo, J. Jaramillo, R. Gomperts, R. E. Stratmann, O. Yazyev, A. J. Austin, R. Cammi, C. Pomelli, J. W. Ochterski, R. L. Martin, K. Morokuma, V. G. Zakrzewski, G. A. Voth, P. Salvador, J. J. Dannenberg, S. Dapprich, A. D. Daniels, O. Farkas, J. B. Foresman, J. V. Ortiz, J. Cioslowski, D. J. Fox: *Gaussian 09*. Revision A.02 ed.; Gaussian, Inc.: Wallingford CT, 2009.
25. R. Krishnan, J. S. Binkley, R. Seeger, J. A. Pople, *J. Chem. Phys.* **1980**, *72*, 650.
26. A. J. H. Wachters, *J. Chem. Phys.* **1970**, *52*, 1033.
27. P. J. Hay, *J. Chem. Phys.* **1977**, *66*, 4377.
28. A. D. McLean, G. S. Chandler, *J. Chem. Phys.* **1980**, *72*, 5639.
29. D. Rappoport, F. Furche, *J. Chem. Phys.* **2010**, *133*, 134105.
30. D. Andrae, U. Haeussermann, M. Dolg, H. Stoll, H. Preuss, *Theor. Chim. Acta* **1990**, *77*, 123.
31. C. Adamo, V. Barone, *J. Chem. Phys.* **1998**, *108*, 664.
32. K. Fukui, *Acc. Chem. Res.* **1981**, *14*, 363.
33. K. Fukui, *J. Phys. Chem.* **1970**, *74*, 4161.
34. C. Gonzalez, H. B. Schlegel, **1990**, *94*, 5523.
35. C. Gonzalez, H. B. Schlegel, *J. Chem. Phys.* **1989**, *90*, 2154.
36. K. Wolinski, J. F. Hinton, P. Pulay, *J. Am. Chem. Soc.* **1990**, *112*, 8251.
37. C. Hansch, A. Leo, R. W. Taft, *Chem. Rev.* **1991**, *91*, 165.
38. M. Manoharan, P. Venuvanalingam, *J. Mol. Struct. (THEOCHEM)* **1997**, *394*, 41.
39. M. Manoharan, P. Venuvanalingam, *J. Chem. Soc., Perkin Trans* **1997**, 1799.
40. K. B. Wiberg, *Tetrahedron* **1968**, *24*, 1083.
41. H. J. Eyring, *Chemical Physics* **1935**, *3*, 107.
42. W. F. K. Wynne-Jones, H. J. Eyring, *Chemical Physics* **1935**, *3*, 492.
43. H. Eyring, *Chemical Reviews* **1935**, *17*, 65.



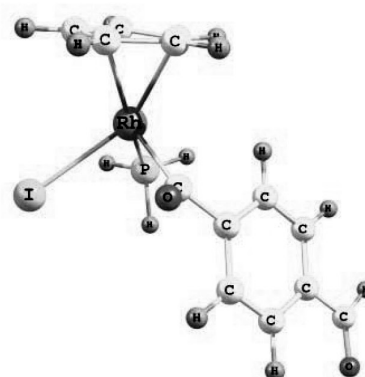
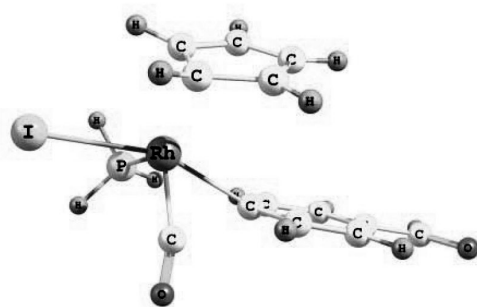
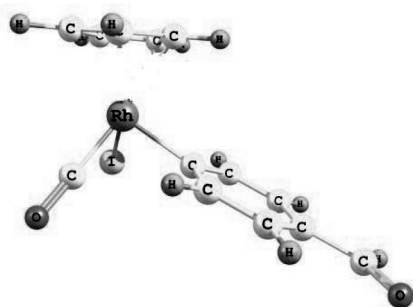
X=H



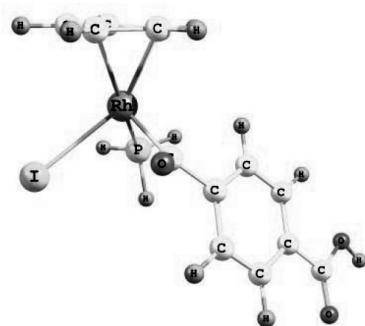
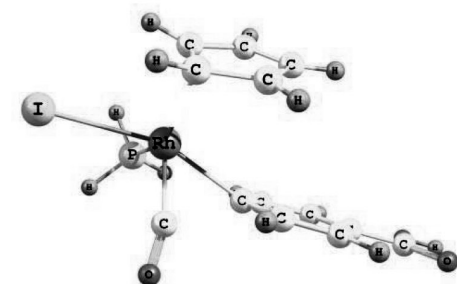
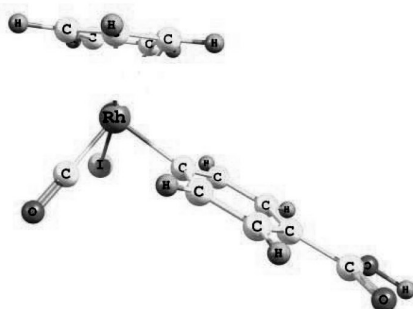
X=F



X=Cl



X=CHO



X=COOH

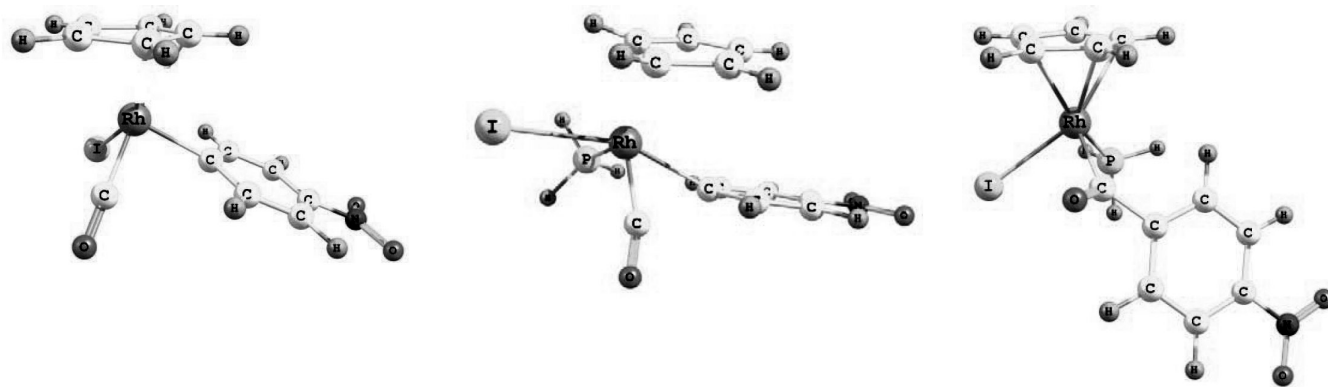


Figure S1. The structures of (I), (TS) and (II).